

# Multicontext wavelet-based thresholding segmentation of brain tissues in magnetic resonance images

Zhenyu Zhou<sup>a,b,\*</sup>, Zongcai Ruan<sup>a</sup>

<sup>a</sup>*Research Center of Learning Science, Southeast University, Nanjing 210096, China*

<sup>b</sup>*School of Biological Science and Medical Engineering, Southeast University, Nanjing 210096, China*

Received 15 June 2006; accepted 22 September 2006

---

## Abstract

A novel segmentation method based on wavelet transform is presented for gray matter, white matter and cerebrospinal fluid in thin-sliced single-channel brain magnetic resonance (MR) scans. On the basis of the local image model, multicontext wavelet-based thresholding segmentation (MCWT) is proposed to classify 2D MR data into tissues automatically. In MCWT, the wavelet multiscale transform of local image gray histogram is done, and the gray threshold is gradually revealed from large-scale to small-scale coefficients. Image segmentation is independently performed in each local image to calculate the degree of membership of a pixel to each tissue class. Finally, a strategy is adopted to integrate the intersected outcomes from different local images. The result of the experiment indicates that MCWT outperforms other traditional segmentation methods in classifying brain MR images.

© 2007 Elsevier Inc. All rights reserved.

**Keywords:** Wavelets; Image segmentation; Magnetic resonance imaging; Brain imaging; White matter; Gray matter; Cerebrospinal fluid

---

## 1. Introduction

Magnetic resonance (MR) imaging is an advanced medical technology in brain anatomy research. It can provide rich information about human brain anatomy in two dimensions in a noninvasive way. White matter (WM), gray matter (GM) and cerebrospinal fluid (CSF) are three basic tissues in the brain. Brain tissue segmentation consists of assigning a label to each pixel of a thin-sliced single-channel brain MR scan. This label indicates which class a pixel belongs to. The goal is to obtain a partition of the image that is composed of homogeneous regions, with each partition representing a class. It is an important preprocessing step in brain research and clinical applications because these contrasts define the boundaries of most brain structures. Currently, many available methods for MR image segmentation have been developed, especially from classical, statistical, fuzzy and neural network techniques

[1–3]. Classical techniques include threshold, edge-based and pixel-based techniques. These approaches extract tissue that is defined by intensity transitions or by gradients of intensity transitions and have been used to manually or semiautomatically outline cortical and subcortical structures [4,5]. Pixel-based methods used in previous publications have been successful in partitioning CSF from brain parenchyma. Then, a threshold is defined based on the histogram of the brain image. Pixels with intensity above the threshold belong to a particular tissue while other pixels belong to the other tissue.

Unfortunately, intensity inhomogeneities in brain MR images, which can change the absolute intensity for a given tissue class in different locations, are a major obstacle to any automatic method for MR imaging segmentation and make it difficult to obtain accurate segmentation results [5]. Traditional thresholding techniques for segmentation based on the histogram of the MR images do not work well because of the presence of random noise and magnetic field inhomogeneities [6]. On the basis of the local image model, the wavelet multiscale transform of local image gray histogram is done and the gray threshold is gradually revealed from large-scale to small-scale coefficients [7,8].

---

\* Corresponding author. Tel.: +86 25 83795664 1003; fax: +86 25 83795929 1005.

E-mail addresses: [oleander@seu.edu.cn](mailto:oleander@seu.edu.cn) (Z. Zhou), [rzc.rcls@seu.edu.cn](mailto:rzc.rcls@seu.edu.cn) (Z. Ruan).

An ideal segmentation method based on wavelet presents overlapping multigrid brain images and is applicable to our large database. It has been applied in a brain imaging toolkit that we developed. It is automated, fast, reliable and valid.

This article is organized as follows. Section 2 presents a local image model instead of a global model. By simplifying the model into its local version, the adverse impact is eliminated. Based on the local model, a new method is presented in Section 3 to classify 2D data effectively and reliably while avoiding the possibility of removing useful information. In Section 4, experimental results on real 2D MR images are presented. The final section is devoted to discussion and conclusions.

## 2. Hypotheses of local image model

The key to our classification model is the idea of local image model. Estimation and correction for inhomogeneities are not necessary because a local version of the model can be deduced to eliminate the adverse effect of intensity inhomogeneities.

With this in mind, the following hypotheses were found to be necessary:

*Hypothesis 1.* There are only pure pixels throughout the putamen area.

*Hypothesis 2.* Within the context of the brain area of the image, the tissues exit together and each tissue's pixels are considerable.

*Hypothesis 3.* All pixels of the same kind of tissues have similar intensities within a context.

*Hypothesis 4.* After preprocessing of the original brain image, there are only GM, WM and little CSF left in the brain area.

## 3. Method

### 3.1. Preprocessing

Images were filtered with 3D anisotropic filters (number of iteration=4,  $k=10$ , no bias) to improve signal-to-noise ratio and the contrast-to-noise ratio of the images [9,10]. The filtering process smoothens out the regions without disturbing the regional boundaries and reduces the variance of the intensities of tissues without altering the means of intensities.

Brain shelling means separating the cerebrum from external skull, bone, dura, brain stem and cerebellum of the MR scans. Based on an active brain template from the head scans, one can obtain the brain area of the image. A brain model composed of separate models of the left and right cerebellum and the cerebrum is used here (Fig. 1).

As the surface wipes off, the earlier selected threshold removes the background pixels and most CSF pixels that are

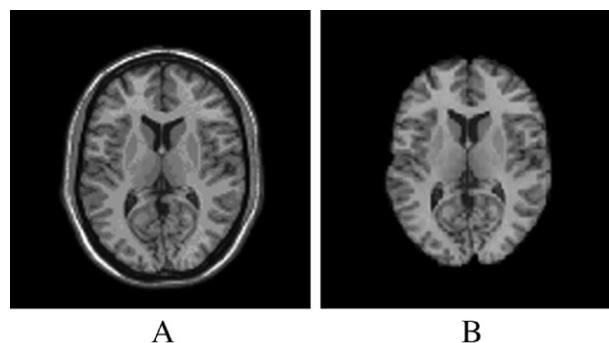


Fig. 1. (A) Original image. (B) Image after filtering and brain shelling.

below the threshold. Therefore, there are only GM, WM and little CSF left in the brain area of the MR scans.

### 3.2. Wavelet-based thresholding segmentation (WTS)

The basic idea of traditional histogram-based thresholding technique is that images consist of regions with different features [3]. The histogram of an image indicates combined probability distributions of constituent tissue types.

The gray-level histogram of an image may have one or more peak values. By choosing one or more thresholds of gray level, the object regions can be classified for further processing. If the histogram has obvious peak values, we can get the thresholds easily. Nevertheless, because of noise in practice, we could not always make a good choice of the threshold. The threshold could easily be influenced by the noise.

A thresholding technique based on wavelet transform can easily avoid the impact of the noise. The essential idea of this method is as follows: first, decompose the gray-level histogram of an image into the wavelet coefficients of different hierarchy by a dyadic wavelet transform; then, select the thresholds depending on the rule of segmentation and the dyadic wavelet coefficients; finally, obtain the hard segmentation via the thresholds. The thresholds of segmentation are gradually revealed from large-scale to small-scale coefficients [8,11].

For every integer  $j \in \mathbb{Z}$  ( $\mathbb{Z}$  is integer union),  $\{d_j = \frac{k}{2^j}, k \in \mathbb{Z}\}$  express binary rational number at the resolution  $j$ . Thus, for any  $j \in \mathbb{Z}$ ,  $d_j$  is a union of equidistant/uniform samples on the real axis; if  $i < j$ , then  $d_i$  indicates samples with low resolution. On the contrary, if  $i > j$ , then  $d_i$  indicates samples with high resolution. We assume that if an image is defined as a function  $f(x, y)$  and  $D_m$  is the gray maximum in the image  $f(x, y)$ , then the histogram can be:  $h_f(k) = |\{(x, y): f(x, y) = k\}|$ ;  $k \in [0, D_m]$ , where “ $|\dots|$ ” is the operation of count and  $h_f(k)$  is the discrete function. Let  $h_f(x) = h_f(k)$ ,  $x \in [k, k+1]$ , then the discrete function  $h_f(k)$  can be the continuous function  $h_f(x)$  and  $h_f(x)$  can be thought of as piecewise constant functions on the interval  $[0, 1]$ . For  $j \in \mathbb{Z}$ , sampling  $h_f$  at samples of  $\{d_j\}$ , then  $h_f^j$  is a

histogram at resolution  $j$ . Now, we need to define the basis for  $h_f^j$ ; it is given by the set of scaled and translated function called Haar scaling function  $\phi(x)$ , such that:

$$\phi(x) = \begin{cases} 1, & \text{if } x \in [0, 1] \\ 0, & \text{otherwise} \end{cases} \quad (1)$$

$$h_f^j(x) = \sum_{n \in \mathbb{Z}} h_f(2^{-j}n) \phi(2^j x - n) \quad (2)$$

Because the continuous function  $h_f(x)$  consists of several piecewise constant functions, we consider using a filter to smooth the function  $h_f(x)$  to eliminate its high-frequency parts.  $h_f(x)$  is described as follows:

$$h_f(x) = \sum_{k \in \mathbb{Z}} a_k \phi_{j,k}, \quad (3)$$

where

$$\{a_k\} = \{\langle h_f, \phi_{j,k} \rangle\}, \phi_{j,k} = 2^{j/2} \phi(2^j x - k). \quad (4)$$

Then, we can easily obtain the corresponding threshold algorithm based on the dyadic wavelet transform.

### 3.3. Multigrid wavelet-based thresholding segmentation (MGWT)

We consider performing WTS in a local manner. It is a natural idea that the nonoverlapping multigrid version of WTS may be better [5]. One context means one grid area here; hence, for one pixel, there is only one context in this method.

This algorithm can prevent the WTS drawback of missing some information, but it is only a single context. Each pixel is completely decided by its local context and cannot obtain information from neighboring contexts. For this reason, MGWT is hypersensitive to the size of the context and it cannot gain spatial continuity segmentation result and statistical reliability. We can see some problems from the hard segmentation result of MGWT applied on a real MR image. The original image is divided into  $4 \times 4$  nonoverlapping regions, as shown in Fig. 2. WTS is implemented independently in every grid area. Then, we

found that the biggest problem is that the variation of intensity distributions of neighboring contexts would lead to incompatible segmentation results across the boundaries of the grid area. Take grid (2,3) and grid (3,3) in Fig. 2B, for example, the segmentations of CSF are obviously wrong.

If we change the size of the context, the result will be consequentially different. Therefore, the determination of the proper size of the context is different in this method because the tissue distributions vary with the different slices and because there are dissimilar contexts in one slice.

For the abovementioned problem, this method could not be used widely.

### 3.4. Multicontext wavelet-based thresholding segmentation (MCWT)

Most contexts could yield good soft judgments in the method of MGWT, although there are some problems, as mentioned above, for the complicated and convoluted structures of the human brain. An idea is that multiple segmentation for each pixel could suppress the adverse impacts [5]. Such a consideration leads to the development of a novel method called the MCWT, which not only can take advantage of MGWT but also can keep the classifications spatially continuous and statistically reliable.

In MCWT, the sharpness of the contexts has to be decided in advance. Here, we select a rectangle for 2D MR images. The only input parameter is the size of the context, which is defined as:

$$\eta = \frac{\|c\|}{n - n_{bk}} = \frac{c_w \times c_h}{I_w \times I_h - n_{bk}}, \quad (5)$$

where  $I_w$  and  $I_h$  are the width and height of the input image and  $n$  is the total pixel number and the number of background pixels whose intensities are zero. Calculation of width  $c_w$  and height  $c_h$  of the rectangular context can be made with the given parameter  $\eta$ . With this definition, the absolute size of the context can be changed with the size of the brain in the original input images. Then, we should pay attention to make sure that these four parameters obey the formula

$$\frac{c_w}{I_w} = \frac{c_h}{I_h}. \quad (6)$$

We move the local window step by step through the whole image with the step length  $S_w$  from left to right and  $S_h$  from top to bottom.

$$S_w = \frac{c_w}{m_w} \quad (7)$$

$$S_h = \frac{c_h}{m_h} \quad (8)$$

In practice,  $m = m_w \times m_h = 3 \times 3$  is enough for 2D images. During the process, each pixel owns  $m$  in different contexts. The calculation is performed along with the movement of

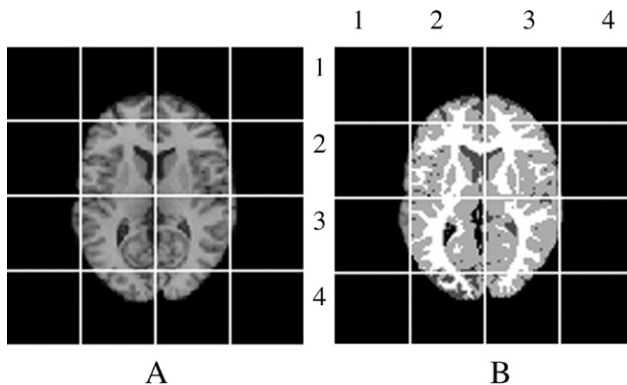


Fig. 2. MGWT hard segmentation. (A) Original  $T_1$ -weighted image. (B) Segmentation result.

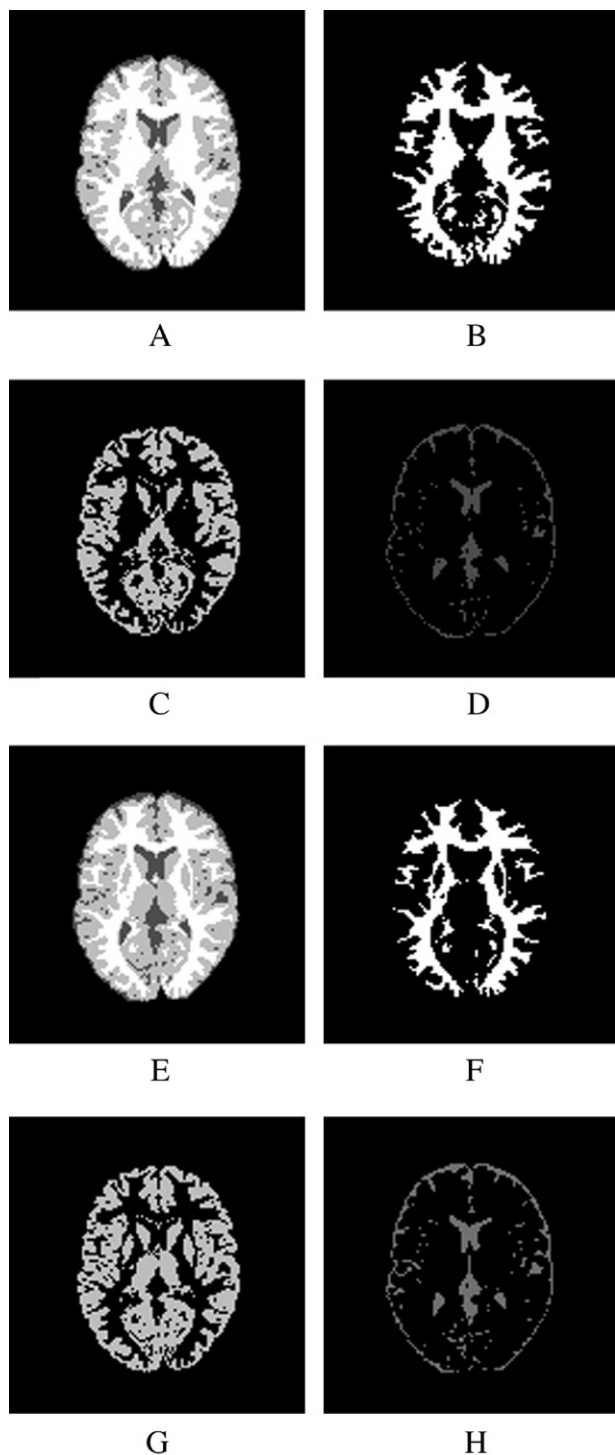


Fig. 3. WTS and MCWT hard segmentation and membership functions. (A) WTS hard segmentation. (B–D) Membership functions of WM, GM and CSF in WTS. (E) MCWT hard segmentation. (F–H) Membership functions of WM, GM and CSF in MCWT.

the rectangular window. For each context, WTS algorithm is done independently. After processing all contexts, the accumulated membership values at each pixel in the accumulated membership maps are divided by the context

number of the corresponding pixels to obtain the weighted averaging membership values.

Finally, the maximum principle is used here to obtain the thresholds for hard segmentation.

#### 4. Results

MCWT was implemented in a C environment on a PC (Intel Pentium IV, 3.0 GHz CPU, and 512 M RAM). It has been tested on real MR images.

Fig. 3 shows the hard segmentation results of WTS and MCWT on real MR images. Obviously, the membership function of WM at the putamen area calculated by WTS misclassified most parts into WM. On the other hand, MCWT was able to obtain a good result, which is much more compatible with human visual perception.

Also, by comparing MCWT and MGWT results (both have the same size of contexts:  $64 \times 64$ ), it can be seen that MCWT has gained spatial continuity segmentation, as shown in Fig. 2. All the above improvements indicate that MCWT is much better than the other two segmentations in classifying WM, GM and CSF of the brain image.

#### 5. Discussion and conclusion

We have developed a fully automatic algorithm to separate GM and WM from high-resolution  $T_1$ -weighted MR images of human brains. It appears valid and reliable and can be used to segment large data sets. Our method fills the need to analyze MR image data sets with thin slices and with more than 150 slices for each brain.

Noise and random errors were eliminated when anisotropic filtering was used, which improved noise and contrast without mixing edges or structural details.

The studies confirmed greater accuracy with the use of MCWT, which is based on a local model, than with the global method and the nonoverlapping MGWT. MCWT could classify brain tissues fast and validly. In addition, the little CSF left after preprocessing can also be classified from the images.

Our technique of segmentation based on wavelet transform could be useful in measuring brain tissues and in finding a correlation of such measurements to behavioral and physiological parameters for clinical populations. The application of brain MR images for the development of the brain of patients with infantile autism is our objective. This algorithm has been added to the brain imaging toolkit that we developed and will be applied to a number of brain scans; also, one can even work with this algorithm via the Internet.

#### References

- [1] Lin Y, Tian J, Zhang X. Application of a new medical image segmentation method based on fuzzy connectedness and FCM. *Chin J Stereology Image Anal* 2001;6(2):103–8.

- [2] Chaozhe Z, Tianzi J. Multicontext fuzzy clustering for separation of brain tissues in magnetic resonance images. *Neuroimage* 2003;18: 685–96.
- [3] Rajapakse JC, Giedd JN, De Carl C, et al. A technique for single-channel MR brain tissue segmentation: application to a pediatric sample. *Magn Reson Imaging* 1996;14(9):1053–65.
- [4] Filipek PA. The young adult human brain: an MRI-based morphometric analysis. *Cereb Cortex* 1994;4(4):344–60.
- [5] Shattuck DW, Sandor-Leahy SR, Schaper KA, Rottenberg DA, Leahy RM. Magnetic resonance image tissue classification using a partial volume model. *Neuroimage* 2001;13:856–76.
- [6] Olivo JC. Automatic threshold selection using the wavelet transform. *CV GIP - Graph Models Image Process* 1994;56(3):205–18.
- [7] Mallat SG, Hwang WL. Singularity detection and processing with wavelets. *IEEE Trans Inf Theory* 1992;38(3):617–43.
- [8] Mallat SG, Zhong S. Characterization of signals from multiscale edges. *IEEE Tran Pattern Anal Mach Intell* 1992;14(7):710–32.
- [9] Perona P, Malik J. Scale space and edge detection using anisotropic diffusion. *IEEE Tran Pattern Anal Mach Intell* 1990;12(7):629–39.
- [10] Gerig G, Kubler O, Kikinis R, Jolesz FA. Nonlinear anisotropic filtering of MRI data. *IEEE Tran Med Imag* 1992;11(2):221–32.
- [11] Mallat SG. *A wavelet tour of signal processing*. 2nd ed. 2001.